# Prediction of the Limit of the Metastable Zone in the "$CaCO_3$–$CO_2$–$H_2O$" System

**H. Elfil**
Chemical Process Laboratory, Institut National de Recherche Scientifique et Technique (INRST), Soliman, 8020, Tunisia

**H. Roques**
Dept. Génie des Procédés Industriels, Institut National des Sciences Appliquées (INSA) de Toulouse, 31077 Toulouse Cedex 4, France

*DOI 10.1002/aic.10160*
*Published online in Wiley InterScience (www.interscience.wiley.com).*

*The surpassing of the solubility product of the anhydrous forms of calcium carbonate—calcite, aragonite, and vaterite—is not sufficient to induce spontaneous precipitation. The existence of a metastable zone, in the nucleation of the calcium carbonate, is still an experimental phenomenon. A thermodynamic demarcation of the metastable zone in the "$CaCO_3$–$CO_2$–$H_2O$" system, where only a secondary nucleation can occur, has been delimited for the first time. Through experimental exploration of a large supersaturation field, results obtained by the bubbling method are treated with the use of thermodynamic data of different varieties of $CaCO_3$. At temperatures ranging between 25 and 60°C, a primary nucleation (spontaneous precipitation) occurs when the ionic activity product of the calco–carbonic solution surpasses the solubility product of $CaCO_3 \cdot H_2O$. No spontaneous nucleation occurs when the ionic activity product stabilizes between the solubility products of calcite and monohydrated calcium carbonate, which means that the solution remains in a metastable state. The metastability can be broken by seeding with calcium carbonate crystals (aragonite in this case) and then the germination is a secondary one. A model for the prediction of the limit of the metastable zone, presented in this report, is in agreement with experimental results.* © 2004 American Institute of Chemical Engineers
*AIChE J,* 50: 1908–1916, 2004
*Keywords: metastability, secondary nucleation, crystallization, Monohydrated calcium carbonate, calcite*

## Introduction

The formation of solid $CaCO_3$ from a supersaturated aqueous salt solution is a complex process of considerable chemical, geochemical, biological, and industrial importance. It has attracted research studies for more than a century (Sheikholeslami, 2003; Reddy and Nancollas, 1971; Greenwald, 1941; Johnson, 1916). However, this phenomenon is still far from being understood, especially the formation of the precursors (Bolze et al., 2002; Reiger et al., 2000) and the demarcation of the metastable zone.

Most scientific investigations of calcium carbonate have focused on calcite, which is the most stable form. A total of six distinct phases have been recognized. Although three of them are anhydrous crystalline polymorphs (calcite, aragonite, and vaterite), the other three are hydrated forms [ amorphous calcium carbonate (ACC), monohydrate calcium carbonate (MCC), and $CaCO_3 \cdot 6H_2O$].

The supersaturation state of the system is not a sufficient condition for spontaneous germination. A certain degree of

Correspondence concerning this article should be addressed to H. Elfil at elfilh@inrst.rnrt.tn.

**Table 1. Unknown Variables and Equilibrium Equations of $CaCO_3$–$CO_2$–$H_2O$ System**

| Phase | Introduced Variables | Equilibrium Equations | |
|---|---|---|---|
| Gas/liquid | $P_{CO_2}$, $(CO_2)$ | $P_{CO_2} = K_H \cdot (CO_2)$ | (1) |
| Liquid | $(HCO_3^-)$ | | |
| | $(H^+)$ | $\frac{(HCO_3^-)\cdot(H^+)}{(CO_2)} = 10^{-K_1}$ | (2) |
| | $(CO_3^{2-})$ | $\frac{(CO_3^{2-})\cdot(H^+)}{HCO_3^-} = 10^{-K_2}$ | (3) |
| | $(OH^-)$ | $(H^+)\cdot(OH^-) = 10^{-K_w}$ | (4) |
| | Electric neutrality of the solution | $2[Ca^{2+}] = [H^+] + [OH^-] + [HCO_3^-] + 2[CO_3^{2-}]$ | (5) |
| Liquid/solid | $(Ca^{2+})$ | $(Ca^{2+})\cdot(CO_3^{2-}) = K_S$ | (6) |

supersaturation must also be reached at which spontaneous nucleation occurs (Elfil, 1999; Gache, 1998; Ogino et al., 1987; Koutsoukos et al., 1984). The existence of the metastable zone in the nucleation of calcium carbonate is still an experimental fact, but the limits of this zone are not agreed on yet. Ulrich and Sterge (2002) and Mersmann (1995) stated that the metastable limit is, in contrast to the supersaturation limit, thermodynamically not found and kinetically not well defined. Also, Ulrich and Sterge (2002), and Mersmann and Bartosch (1998) indicated that in a few cases, the metastable zone width is located. Nielsen and Toft (1984) and Mulin (1993) earlier defined it as the zone located between the solubility and the supersolubility curves. Elfil and Roques (1999) previously defined the metastable zone in the "$CaCO_3$–$CO_2$–$H_2O$" system as a supersaturation subregion located between the precipitation straight-line limit (PSL), which is obtained experimentally, and the equilibrium curve of the least soluble variety of $CaCO_3$, which is calcite.

During crystallization, a system goes through different distinguishable phases. The first phase is evidently nucleation, which constitutes the priming of the ordered stacking characteristic of the future crystal. Nucleation is categorized as either primary or secondary. Primary nucleation occurs spontaneously without the presence of any crystalline matter. In contrast, secondary nucleation requires the presence of crystals interacting with the environment (Mulin, 1993). Primary nucleation can be classified as homogeneous (if it occurs in the core of the solution) or heterogeneous (if it is induced by contact with partition or suspension of foreign particles).

To suppress primary nucleation of calcite in growth experiments and obtain only a secondary heterogeneous germination, Tai et al. (1999) carried out more than 50 experiments to demarcate the metastable region for calcium carbonate at pH = 8.5 and $t = 25$°C. For Collier and Hounslow (1999), only a very slight primary nucleation occurred in a seeded batch system where seed crystals were added to a metastable solution.

In this work, the metastable zone of $CaCO_3$–$CO_2$–$H_2O$ system is thermodynamically delimited for the first time. The thermodynamic data for all the varieties of calcium carbonate are taken into account in the analysis of the experimental data obtained by the air-bubbling technique (Roques and Girou, 1974). A model for demarcation of metastable region is presented in this report, and compared to the experimental results of Tai et al. (1999).

## Theory

Unlike other systems, the $CO_2$–$H_2O$–$MeCO_3$ system has three phases. The unknown variables and equations available for studying the calco–carbonic system are summarized in Table 1 (Roques, 1996). Table 1 shows that for a constant temperature (fixed variable), there are seven unknown variables and only six independent equations. This means that the system is bivariant. The phase rule ($\nu = 2 + n - \varphi$) leads to the same conclusion (that is, system is bivariant), given that there are three independent constituents ($n = 3$ for [$CO_2$, $H_2O$, $MeCO_3$]) and three phases ($\varphi = 3$).

Having a constant temperature reduces the complexity of the equations in Table 1. If the temperature were also a variant, the system of equations would need to account for the dependency of the constants in Table 1 on temperature. These constants include:

- Solubility products
- Dissociation constants ($K_1$, $K_2$)
- $CO_2$ solubility in liquid phase
- Constants involved in the count of the ionic strength and activity coefficient

Because the number of additional unknown variables and the number of equations dependent on temperature is equal to the number of dependent constants, the system remains bivariant and it becomes more complicated to understand and analyze.

The equilibrium of the Me–carbonic system can be described in terms of two principal variables, one being expressed in terms of the other. The logical choice of variable for understanding the linkage between cause and effect is obviously {$P_{CO_2}$, [$Me^{2+}$]}, where the first represents the potential aggressivity of the solution and the second, the amount of solid that has moved into liquid when equilibrium is achieved. This approach appears to be the most instructive in terms of acquiring a physical interpretation of the various equilibrium states.

In case the liquid and gas phases are in equilibrium vis-à-vis $CO_2$ exchange, the $P_{CO_2}$ variable can be substituted by the easier measurable pH. If this is not the case, the system may correspond to a partial equilibrium between dissolved species. Partial equilibrium is susceptible to any variation of $CO_2$ exchange between the gas and liquid phases, and the $P_{CO_2}$ variable cannot be substituted by pH. However, many research works concerned with aqueous equilibrium forget this simple truth. Then, the analysis of their work is performed by applying {pH, [$Me^{++}$]} equilibrium diagrams to represent system behavior in spite of its limitation. In this report, we will avoid this limitation by implicitly assuming that the gas and liquid phases

**Table 2. Logarithmic Solubility Products for the Various Forms of Calcium Carbonate**

| Variety | Equations of p$Ks$ ($T$ in $K$ and $t$ in °C) | | Reference |
|---|---|---|---|
| Calcite | $171.9065 + 0.077993T - 2839.319/T - 71.595 \log(T)$ | $0 < t < 90$°C | Plummer and Busenberg (1982) |
| Aragonite | $171.9773 + 0.077993T - 2903.293/T - 71.595 \log(T)$ | $0 < t < 90$°C | Plummer and Busenberg (1982) |
| Vaterite | $172.1295 + 0.077996T - 3074.688/T - 71.595 \log(T)$ | $0 < t < 90$°C | Plummer and Busenberg (1982) |
| ACC | $6.1987 + 0.0053369t + 0.0001096t^2$ | $10 < t < 55$°C | Brecevic and Nielsen (1993) |
| $CaCO_3 \cdot H_2O$ | $7.05 + 0.000159t^2$ | $10 < t < 50$°C | Kralj and Brecevic (1995) |
| $CaCO_3 \cdot 6H_2O$ | $2011.1/T - 0.1598$ | $0 < t < 25$°C | Bischoff et al. (1993) |

are in equilibrium with respect to $CO_2$ exchange at the moment the pH measurement is made.

The supersaturation $\Omega$ is calculated with respect to one of the varieties of calcium carbonate using Eq. 7. The different equations of solubility product are given in Table 2

$$\Omega = \frac{\text{IAP}}{Ks} = \frac{(Ca^{2+})(CO_3^{2-})}{Ks} \tag{7}$$

where

$$(Ca^{2+}) = \gamma_{Ca^{2+}}[Ca^{2+}] \tag{8}$$

and

$$(CO_3^{2-}) = \gamma_{CO_3^{2-}}[CO_3^{2-}] = \frac{1}{2}(2[Ca^{2+}] + [H^+] - [OH^-] - [HCO_3^-]) \tag{9}$$

Individual ion activity coefficients ($\gamma_i$) are calculated by using the method of Truesdell and Jones (1974), which is based on a modified form of the Debye–Hückel equation. The Truesdell–Jones model is used for nonconcentration solution with ionic strength less than 0.2 (the ionic strength of our solutions will never exceed 0.02). In a famous report of their investigation of the $CaCO_3$–$CO_2$–$H_2O$ system, Plummer and Busenberg (1982) demonstrated that the Truesdell–Jones model is adequate for Ca–carbonic solution with a concentration $< 25$ mmol/L

$$\log(\gamma_i) = \frac{A\nu_i^2\sqrt{\mu}}{1 + Ba_i\sqrt{\mu}} + b_i\mu \tag{10}$$

where $\mu$ is ionic strength, $A$ and $B$ are constants defined by Harmer (1968), and $a_i$ and $b_i$ are parameters assigned by Truesdell and Jones (1974).

By combining Eq. 9 with Eqs. 2 and 3, we obtain

$$(CO_3^{2-}) = (HCO_3^-)10^{\text{pH}-K_2} = (CO_2)10^{2\text{pH}-K_1-K_2} \tag{11}$$

Equation 11 allows the relative proportions of $CO_2$, $HCO_3^-$, and $CO_3^{2-}$ as a function of pH, to be calculated as follows

$$[CO_2]\% = \frac{100}{1 + \dfrac{10^{\text{pH}-K_1}}{\gamma_{HCO_3^-}} + \dfrac{10^{2\text{pH}-K_1-K_2}}{\gamma_{CO_3^{2-}}}} \tag{12}$$

$$[HCO_3^-]\% = \frac{100\dfrac{10^{\text{pH}-K_1}}{\gamma_{HCO_3^-}}}{1 + \dfrac{10^{\text{pH}-K_1}}{\gamma_{HCO_3^-}} + \dfrac{10^{2\text{pH}-K_1-K_2}}{\gamma_{CO_3^{2-}}}} \tag{13}$$

$$[CO_3^{2-}]\% = \frac{100\dfrac{10^{2\text{pH}-K_1-K_2}}{\gamma_{CO_3^{2-}}}}{1 + \dfrac{10^{\text{pH}-K_1}}{\gamma_{HCO_3^-}} + \dfrac{10^{2\text{pH}-K_1-K_2}}{\gamma_{CO_3^{2-}}}} \tag{14}$$

Also, Eqs. 1 and 2 can be combined to yield $CO_2$ partial pressure as

$$P_{CO_2} = K_H \cdot (CO_2) = [HCO_3^-]\gamma_{HCO_3^-}10^{K_1-\text{pH}} \tag{15}$$

where $K_H$, $K_1$, and $K_2$ are, respectively, the Henry low coefficient and the first and second dissociation constants of the carbonic acid; their values (Plummer and Busenberg, 1982) are summarized in Table 3.

## Experimental studies

The experimental results of this study were obtained using the setup shown in Figure 1. These results will be used to introduce our findings of $CaCO_3$ precipitation. The method consists of displacing the equilibrium of $Ca(HCO_3)_2$ solution by bubbling it with a $CO_2$–air mixture. The $CO_2$ partial pressure ($P_{CO_2}$) of the bubbling gas is set lower than the equilibrium $P_{CO_2}$ of the Ca–carbonic solution, leading to a supersaturation state. The magnitude of the supersaturation can be

**Table 3. Values of Henry's Law Coefficient ($K_H$) and First and Second Dissociation Constants ($K_1$, $K_2$) of Carbonic Acid**

| | Temperature, $T$ (°C) | | | | |
|---|---|---|---|---|---|
| Variable | 25 | 30 | 40 | 50 | 60 |
| $K_H \times 10^{-5}$ (Pa L mol$^{-1}$) | 22.549 | 33.769 | 42.586 | 51.920 | 61.476 |
| $K_1$ | 6.4 | 6.37 | 6.34 | 6.32 | 6.33 |
| $K_2$ | 10.35 | 10.31 | 10.24 | 10.19 | 10.16 |

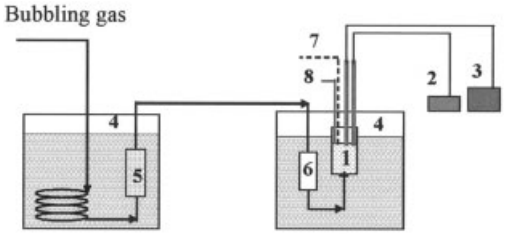


**Figure 1. Experimental setup used for studying $CaCO_3$ precipitation kinetics.**

adjusted by varying the initial concentration of the solution, $P_{CO_2}$ of the bubbling gas, or temperature.

The setup consists of a thermally controlled reactor containing a solution with known $CaCO_3$ concentration. An electrode allows pH to be recorded. Also, an opening in the cover of the setup is used to remove a sample for determining the amount of calcium remaining in solution, or to insert a rod to capture crystals for microscope and X-ray diffraction examination. A gas mixture (air–$CO_2$) is introduced in the system through a distributor located at the base of the reactor, which causes rapid equilibrium to be achieved vis-à-vis $CO_2$ in the gas phase. Because bubbles may cause homogenization of the solution (as would be made by mechanical agitation), the gas distributor is carefully positioned to avoid an insulating gas girdle formation in contact with the pH electrode.

During each experimental run, the pH and [Ca] and/or [Alc] were recorded while $CO_2$ was bubbling through the solution. A high $P_{CO_2}$ gas is used at the beginning of an experiment to produce a highly undersaturated system to eliminate any crystal seed which may exist in solution. The Ca–carbonic solution is prepared by bubbling pure $CO_2$ in an aqueous suspension of $CaCO_3$.

A computer model was developed to solve the equilibrium equations in Table 1 of the $CaCO_3$–$CO_2$–$H_2O$ system. The inputs to the model include experimental data recorded for pH and [Ca] at fixed temperature, and the outputs consist of $P_{CO_2}$, ionic activity product (IAP), and supersaturation ($\Omega$) of the solution. The final results of the computer code are experimental curves similar to those shown in Figure 2.

## Results and Discussion

### *Curves for $CaCO_3$ precipitation obtained by the air-bubbling method*

Figures 2a and 2b show the schematic evolution of variables during the precipitation process. Note that the time scale for Figures 2a and 2b starts at the initiation of precipitation, and it is assumed to correspond to the moment the bubbling gas is introduced into the reactor. Diagrams of Figures 2a and 2b are observed when a strong supersaturation is created by using a low-enriched $CO_2$ bubbling gas ($P_{CO_{2\text{-Air}}} \sim 30$ Pa) and/or an elevated initial [Ca]. In these conditions, after a regular increase of the solution pH that translates the induced progressive bubbling by the gas passage, a decrease of pH is observed at the initial stage of precipitation ($t_G$ in Figure 2a). This sudden decrease in pH is generally interpreted in the following way:

Under normal work conditions, the initial Ca–carbonic solution has a pH lower than $(pK_1 + pK_2)/2$ ($\cong$ 8.4 at 25°C; Roques, 1996). At this pH the $HCO_3^-$ ions are very predominant relative to the $CO_3^{2-}$ ions in the solution. This would likely explain why the crystalline growth of the crystal is developed between a $Ca^{2+}$ ion and an ion $HCO_3^-$ and not between $Ca^{2+}$ ion and $CO_3^{2-}$ ion. The transformation of $HCO_3^-$ ions to $CO_3^{2-}$ is then necessary before integration into the crystal, according to

$$HCO_3^- + H_2O \rightarrow CO_3^{2-} + H_3O^+ \qquad \text{(R1)}$$

Reaction R1 yields protons ($H_3O^+$) responsible for the decrease in the observed pH. Freeing up protons is also necessary on stoichiometric grounds. Indeed, to satisfy the charge neutrality, a $Ca^{2+}$ ion is associated with two $HCO_3^-$ ions, which means two atoms of C in the solution, whereas in the crystal, a $Ca^{2+}$ ion is associated with a $CO_3^{2-}$ ion, which means only one atom of C. Therefore it is necessary to eliminate the second atom of C, and this happens by the following reaction:

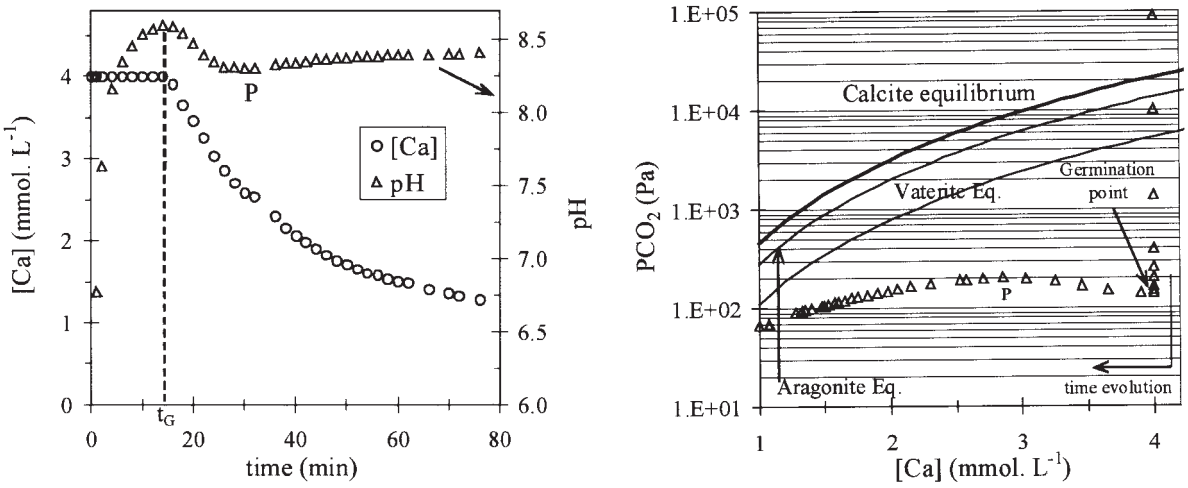


**Figure 2. (a) Typical curves obtained with the experimental setup shown in Figure 1 at fixed temperature (30°C). (b) Representation of the evolution of the system point during the course of an experiment.**

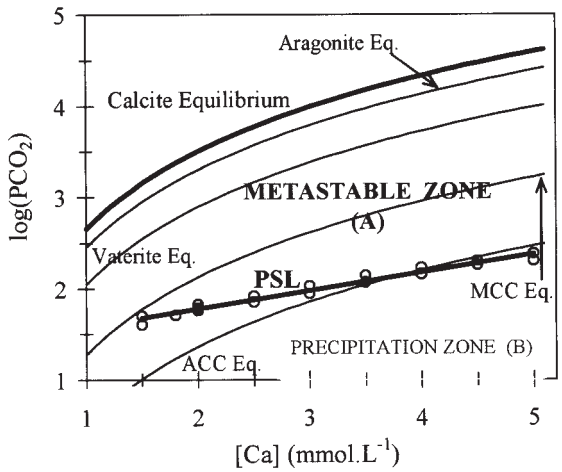


**Figure 3. Metastable zone and PSL position (germination points).**

$$HCO_3^- + H_3O^+ \rightarrow CO_2^{\nearrow} + 2H_2O \qquad (R2)$$

The $CO_2$ production is responsible for the immediate increase in $P_{CO_2}$ equilibrium after the start of the precipitation (Figure 2b). At this moment, the production rate of the proton $H_3O^+$ (R1) is higher than that of $CO_2$ release. This causes an accumulation of $CO_2$ in solution (R2) in excess of its elimination by air bubbling. The precipitation rate decreases thereafter, whereas the bubbling rate remains constant. Later, $CO_2$ bubbling becomes faster than its accumulation and then the pH of the solution begins to increase (point P on Figures 2a and 2b).

### *Precipitation straight-line limit (PSL)*

In a previous work (Elfil and Roques, 1999), with respect to kinetics study of $CaCO_3$ precipitation in an interval of hardness going from 1 to 5 mM, the data points that represent the experimental germination point in the graph {log $P_{CO_2}$·[Ca]} were grouped around a straight line. This line has been called "precipitation straight-line limit" (PSL), which separates the study graph into two zones, as shown in Figure 3:

(1) For data points of the system situated below this PSL (zone B), primary nucleation appears after a long or short time (see Table 4).

(2) For data points situated between this PSL and the equilibrium curves of the anhydrous forms (zone A in Figure 3), no spontaneous precipitation appears after a long time (on the scale of laboratory time). The Ca–carbonic solution conserves a metastability.

The physical significance of this straight line (PSL, Figure 3), is not obvious. Nevertheless, the PSL is asserted to be distinct from equilibrium curves of crystallographic varieties obtained at the same temperature. The PSL does not correspond to the position of points, giving a constant value of the IAP "$(CO_3^{2-})(Ca^{2+})$" or "$(HCO_3^-)^2(Ca^{2+})$" that could correspond to an intermediary unsteady variety and thus, according to the rule of Ostwald, is more soluble.

Independently of its physical significance, this straight line constituted a new and very important element from a practical viewpoint because it represented the limit of the metastability field beyond which spontaneous precipitation occurs.

Some research work on hydrated $CaCO_3$ characterization (Elfil and Roques, 2001a; Gal et al., 2000, 2002) confirm a precursor role of hydrated forms in the germination of calcium carbonate. These observations incited us to evaluate the role of the ACC and MCC precursors in identifying the metastability and the physical significance of PSL. The $CaCO_3$·$6H_2O$ is not considered in the study because of its instability above 6°C (Bischoff et al., 1993). The hexahydrated form is synthesized only near 0°C.

In Figure 3, the position of the PSL is compared to the equilibrium curves for all $CaCO_3$ varieties, except the hexahydrated form. It is clear that the PSL is located between equilibrium curves of amorphous $CaCO_3$ and $CaCO_3$·$H_2O$. This result is obtained at different temperatures between 25 and 60°C.

### *Demarcation of the metastable zone*

Under some experimental conditions (low concentration, high value of $P_{CO_2}$, or weak value of pH) no spontaneous precipitation is observed after a long period of time and the solution remains in a metastable state. Under such conditions, the maximum value of $P_{CO_2}$ is between the equilibrium curves of the $CaCO_3$·$H_2O$ and the calcite as shown in Figure 4. The metastable solutions are supersaturated with respect to the anhydrous forms (calcite, aragonite) and undersaturated in relation to the monohydrated calcium carbonate ($\Omega_{MCC} < 1$).

The region located between the equilibrium curves of $CaCO_3$·$H_2O$ and the most stable form of $CaCO_3$ can be considered as the metastable zone. To confirm the metastable zone width and its relation with the solubility product of MCC, all experiments at 30°C, where spontaneous nucleation takes place, are represented in the graph {IAP–time} independently of the partition nature. Ionic activity products at the germination points ($IAP_G$) are compared to the solubility product of the different varieties of $CaCO_3$. As shown in Figure 5, all the $IAP_G$ values are superior to the solubility product of the monohydrated calcium carbonate. When the experimental conditions are similar (that is, PVC), the germination time is highly dependent on the $IAP_G$. Indeed, the more the $IAP_G$ value approaches the solubility product of MCC the more the germi-

**Table 4. Time, pH, $P_{CO_2}$ and Supersaturation Values on Germination Points for Spontaneous Precipitation ($T$ = 30°C)**

| [Ca] (mmol $L^{-1}$) | $t_G$ (min) | pH | $P_{CO_2}$ (Pa) | Ω (/calcite) | Ω (/$CaCO_3$ · $H_2O$) |
|---|---|---|---|---|---|
| 5.0 | 11 | 8.51 | 210 | 172.3 | 8.4 |
| 4.0 | 16 | 8.59 | 140 | 133.4 | 6.5 |
| 3.0 | 22 | 8.68 | 87 | 94.0 | 4.6 |
| 2.5 | 32 | 8.72 | 66 | 74.6 | 3.6 |
| 2.0 | 44 | 7.54 | 70 | 39.4 | 1.9 |
| 1.5 | 120 | 8.56 | 59 | 21.8 | 1.1 |
| 1.0 | >1000 | 8.58 | 39 | 10.5 | 0.5 |

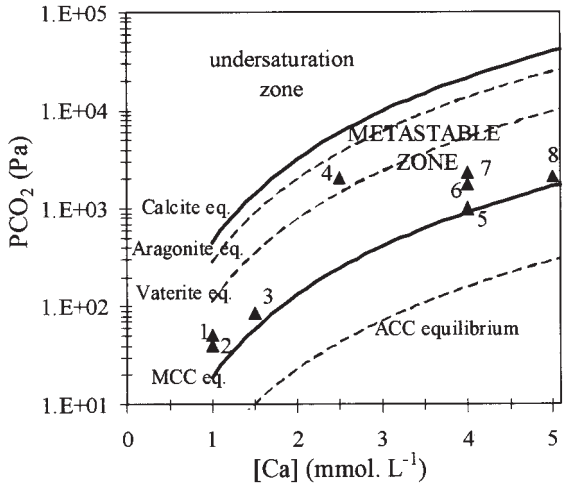


**Figure 4. Position of the nongermination points in relation to equilibrium curves of $CaCO_3$ varieties at 30°C.**

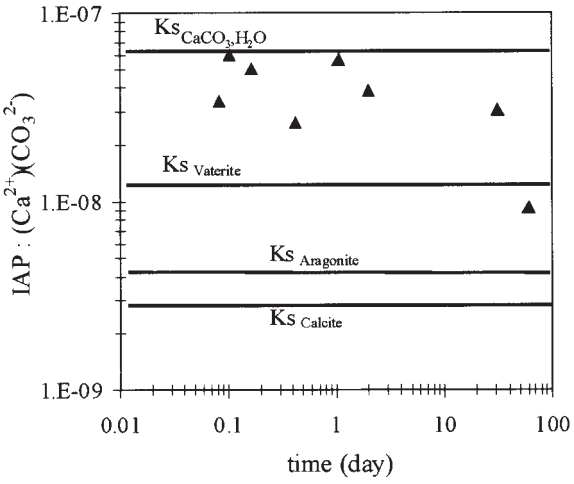


**Figure 6. Position of the IAP solutions, without any precipitation, in relation to equilibrium curves of $CaCO_3$ varieties at 30°C.**

nation time increases. On the contrary, when the $IAP_G$ value approaches the solubility product of ACC the germination time becomes shorter.

In no case is germination observed with an IAP value lower than the solubility product of $CaCO_3 \cdot H_2O$. All of the nongermination experimental results are presented in Figure 6. Compared to the solubility product of the different varieties of $CaCO_3$, the maximum values of IAP reached by the solution are located between calcite and $CaCO_3 \cdot H_2O$. The experimental times have been varied from a few hours to 60 days without any occurrence of spontaneous precipitation.

To summarize, the metastability of a Ca–carbonic solution, which corresponds to a supersaturated solution in relation to calcite without any spontaneous germination occurring, can be defined as: the zone where the solution IAP "$(Ca^{2+})(CO_3^{2-})$" is located between the solubility product of calcite and that of monohydrated calcium carbonate.

### *Exploration of the metastable zone*

Let us first consider point 5 of Figure 4. The solution ([Ca] = 4 mmol $L^{-1}$) is bubbled by an air–$CO_2$ mixture ($P_{CO_2}$ = 980 Pa). After a few minutes, the ionic activity product stabilizes at a value slightly under the solubility product of $CaCO_3 \cdot H_2O$ (Figure 7, curve A). After 150 min of bubbling, the calcium concentration always remains constant with no occurrence of nucleation. A seeding with calcium carbonate (aragonite needles, Figure 8) unblocks the metastability and releases the precipitation. Under these experimental conditions, only a secondary nucleation has been witnessed. As shown in SEM microphotographs (Figures 9 and 10), seeds of aragonite support the germination.

When the operating conditions lead to a primary germination, the crystal formation starts by the amorphous variety (IAP = $Ks_{ACC}$; Elfil and Roques, 2001a) or the monohydrated one ($Ks_{MCC} < IAP < Ks_{ACC}$). The hydrated varieties initially

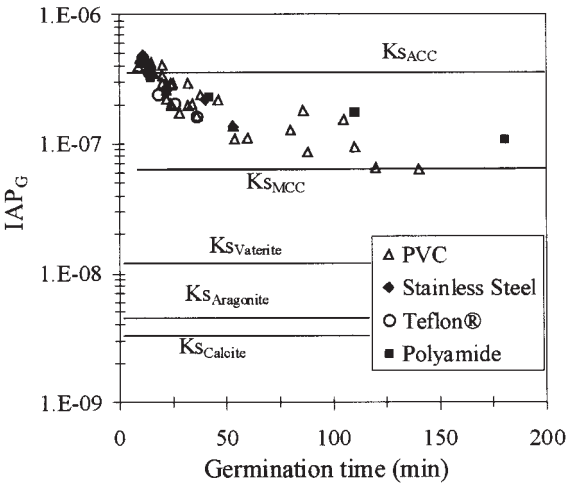


**Figure 5. Position of primary nucleation points with respect to equilibrium curves of $CaCO_3$ varieties at 30°C.**

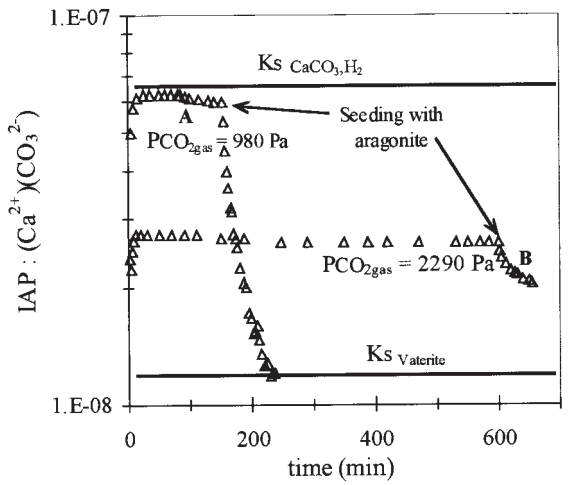


**Figure 7. Evolution of the IAP in the metastable zone and precipitation induced with seeding at 30°C.**

Case 1: $P_{CO_{2gas}}$ = 980 Pa; case 2: $P_{CO_{2gas}}$ = 2290 Pa.

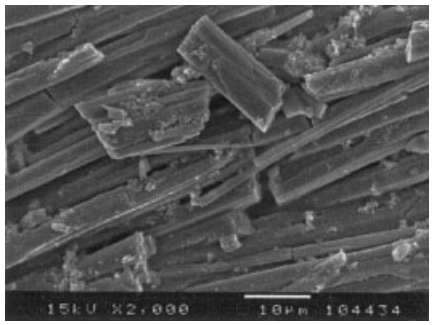


**Figure 8. Seeds of aragonite before seeding.**

formed are transformed to a mixture of several crystalline calcium carbonate polymorphs within a few minutes (Figure 11). The transformed polymorphs depend on many factors that selectively orient the crystallization into one or other varieties.

The second example chosen corresponds to point 7 of Figure 4. A similar Ca–carbonic solution ([Ca] = 4 mmol $L^{-1}$) is bubbled by a mixture gas with $P_{CO_2}$ = 2290 Pa. The IAP is stabilized in the metastable zone for 10 h without nucleation of $CaCO_3$. After seeding with aragonite, the IAP decreases, indicating the start-up of precipitation (Figure 7, curve B). As in the previous experiment, germination is supported by aragonite.

The precipitation kinetic is less important than the preceding one. Indeed, in the first case (point 5) the IAP at the seeding moment is slightly lower than the solubility product of MCC, whereas the IAP of point 7 is much lower. The kinetic of a supported nucleation is more important when the $IAP_G$ is nearing the solubility product of $CaCO_3 \cdot H_2O$ (see Table 5).

To closely examine this observable phenomenon, three experimental runs were conducted with the same amount of seeds. The values of the kinetic constants ($Kc$) of $CaCO_3$ precipitation, at the metastable area, are presented vs. the differences "$IAP_G - Ks_{Aragonite}$" and "$Ks_{CCM} - IAP_G$". A second-order model has been chosen to describe the precipitation kinetic with respect to aragonite. This model was used by Reddy and Nancollas (1971) to study the kinetic of calcite crystals growth from stable supersaturation solution inoculated with calcite seeds

$$\frac{1}{[Ca] - [Ca]_{Eq}} - \frac{1}{[Ca]_0 - [Ca]_{Eq}} = Kc \cdot t \qquad (16)$$


**Figure 9. Aragonite seeds after germination induced by seeding.**

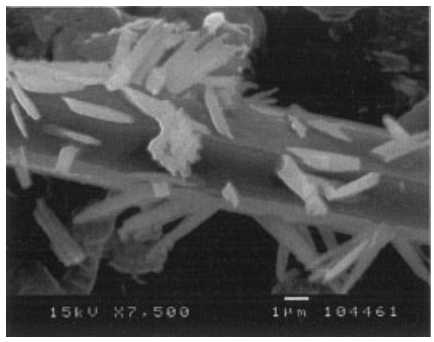


**Figure 10. Germination supported by one seed of aragonite.**

where Eq and 0 are the indexes for equilibrium and initial states, respectively.

The constant of the reaction kinetic is subject to multiple influences that are not well known and difficult to control. Obtained experimental results are given, although the aim of the study was not to have a kinetic aspect. Let us note also that the second-order reaction is a model: the observed kinetic superimposes a chemical reaction and crystalline growth.

It is clear, as shown in Table 5, that the kinetic constants increase as a function of the difference between $IAP_G$ and the solubility product of aragonite. In this case "$IAP_G - Ks_{Aragonite}$" represents the driving force for a secondary nucleation induced by seed crystals of aragonite.

To protect the reactor wall against scaling, a $CaCO_3$ secondary germination without primary nucleation is often looked for (Collier and Hounslow, 1999). However, it is more efficient to use a solution with a high driving force at the seeding moment without exceeding the MCC solubility product. This can be accomplished when the $IAP_G$ of the solution is slightly lower than the solubility product of $CaCO_3 \cdot H_2O$.

### *Comparison of predicted results to experimental ones*

In this section, our model is compared to the experimental results obtained by Tai et al. (1999) for the demarcation of the metastable region. The comparison is presented in Table 6.

Part of this table is borrowed from Tai et al. (1999) (100 mL of $CaCl_2$ and $Na_2CO_3$ solutions were mixed and stirred for 2 h). The authors used "T" and "C" for precipitation and no nucleation, respectively. The supersaturation values in relation to $CaCO_3 \cdot H_2O$ of Tai et al.'s solutions, computed by our computer model, are added to their results in Table 6.

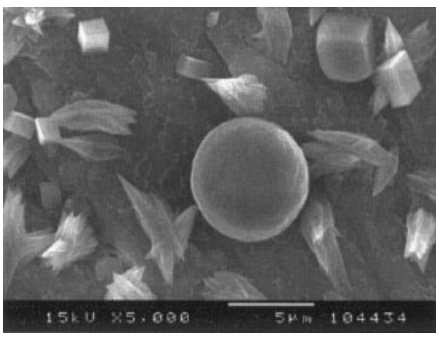


**Figure 11. Mixture of vaterite, aragonite, and calcite.**

**Table 5. Evolution of the Kinetic Constants of $CaCO_3$ Precipitation, after Seeding in the Metastable Zone, vs. the Difference between $IAP_G$ and *Ks* of Aragonite**

| Point | $IAP_G - Ks_{Aragonite}$ | $Ks_{CCM} - IAP_G$ | *Kc* (2nd order) (mmol $L^{-1}$ $min^{-1}$) | $R^2$ |
|---|---|---|---|---|
| 5 | 5.6E-10 | 0.4E-10 | 4.8E-3 | 0.985 |
| 6 | 4.4E-10 | 1.6E-10 | 2.8E-3 | 0.977 |
| 7 | 2.2E-10 | 3.8E-10 | 0.2E-3 | 0.991 |

As shown previously, there is no possibility of spontaneous nucleation if $\Omega_{CCM} < 1$. Comparing the predicted results to the experimental results found by Tai et al., there were only eight cases out of 50 where the experimental results found by Tai and colleagues are in disagreement with the predictions.

The difference can be classified into two categories:

(1) $\Omega_{CCM} > 1$, and C

(2) $\Omega_{CCM} < 1$, and T

*First Case (underlined values).* The solution is slightly supersaturated ($1 < \Omega_{CCM} < 1.3$) in relation to $CaCO_3 \cdot H_2O$. It is possible that nucleation would be delayed beyond 2 h, the time that Tai et al. had fixed for their experiments. Indeed, for a low supersaturated solution, the germination time would be high and would easily exceed 2 h (Elfil and Roques, 2001b).

*Second Case (two values in boldface).* The two values correspond to low alkalinity (=0.0004 mol/L). This disagreement can be explained as follows.

On the one hand, Tai et al. did not report in their study whether the water used was free of $CO_2$. At pH 8.5, $CO_2$ in solution turns into $HCO_3^-$, which is partially transformed to $CO_3^{2-}$ (Roques, 1996), causing an increase in the IAP. The real supersaturation would be higher than the calculated one. On the other hand, the $P_{CO_2}$ corresponding to the two solutions (A: $[CaCl_2]$ = 25 mmol/L and $[Na_2CO_3]$ = 0.25 mmol/L; B: $[CaCl_2]$ = 15 mmol/L and $[Na_2CO_3]$ = 0.4 mmol/L) are 8.6 and 14.4 Pa, respectively, which are much less than the $P_{CO_2}$ of atmospheric air (30 Pa; Elfil, 1999). Then, by stirring the low-enriched $CO_2$ solution, it could absorb $CO_2$ from atmospheric air and, consequently, the alkalinity and the real supersaturation would increase.

## Conclusion

Three fields can characterize the "$CaCO_3$–$CO_2$–$H_2O$" system as shown in Figure 12:

(1) *Undersaturation zone*, in relation to the most stable variety (calcite), where there is no thermodynamic possibility of $CaCO_3$ precipitation (zone C).

(2) *Primary nucleation or spontaneous precipitation zone* (B), which corresponds to supersaturated solutions in relation to monohydrated calcium carbonate. In a previous work, Elfil and Roques (2001a,b) highlighted a predominantly heterogeneous germination when the IAP of solution stabilizes between *Ks* values of monohydrated and amorphous forms. On the contrary, in the case where the solubility product of the ACC is surpassed, germination seems to be predominantly homogeneous.

(3) *Metastable zone*, located between the two previous zones, corresponds to the region between the equilibrium curves of calcite and $CaCO_3 \cdot H_2O$ (zone A). At this zone the solution is supersaturated with respect to calcite and undersaturated with respect to the monohydrated form. This means that

**Table 6. Demarcation of Metastable Region for $CaCO_3$ at pH = 8.5 and $T$ = 25°C***

| | $[CaCl_2]$ (mol/L) | | | | | | |
|---|---|---|---|---|---|---|---|
| $[Na_2CO_3]$ (mol/L) | 0.05 | 0.025 | 0.015 | 0.005 | 0.0025 | 0.0015 | 0.0005 |
| 0.05 | | | | | | | 2.85 T |
| 0.025 | | | | | | | 1.82 T |
| 0.0175 | | | | | | | 1.43 T |
| 0.015 | | | | | | | 1.28 C |
| 0.005 | 24.35 T | | | 4.60 T | 2.64 T | 1.60 T | 0.56 C |
| 0.004 | | | | | | 1.34 T | |
| 0.0035 | | | | | | 1.18 T | |
| 0.00325 | | | | | | 1.11 C | |
| 0.003 | | | | | 1.64 T | 1.03 C | |
| 0.0025 | 12.25 T | | | 2.64 T | 1.38 T | 0.86 C | |
| 0.00225 | | | | | 1.25 C | | |
| 0.002 | | | | | 1.11 C | | |
| 0.0015 | | | | 1.51 T | 0.85 C | | |
| 0.00125 | 6.14 T | | | | | | |
| 0.001 | | | | 1.04 C | | | |
| 0.000875 | 4.32 T | | | | | | |
| 0.0005 | 2.47 T | 1.59 T | 1.14 T | 0.52 C | 0.57 C | | |
| 0.00045 | 2.22 T | | | | | | |
| 0.0004 | 1.97 T | 1.27 T | **0.91 T** | 0.42 C | | | |
| 0.000375 | | | 0.85 C | | | | |
| 0.00035 | 1.73 T | 1.11 T | | | | | |
| 0.0003 | | | 0.68 C | | | | |
| 0.00025 | 1.23 T | **0.79 T** | 0.57 C | | | | |
| 0.000225 | 1.12 T | 0.71 C | | | | | |
| 0.0002 | 0.98 C | 0.63 | | | | | |
| 0.00015 | 0.73 C | | | | | | |
| 0.00005 | 0.24 C | | | | | | |

*T, turbid; C, clear (Tai et al., 1999). Numerical values: supersaturation in relation to $CaCO_3 \cdot H_2O$ (calculated by our code). Turbid means precipitation of $CaCO_3$; clear means no precipitation after 2 h. $\Omega_{CCM} > 1$: spontaneous precipitation of $CaCO_3$; $\Omega_{CCM} < 1$: no spontaneous precipitation of $CaCO_3$.

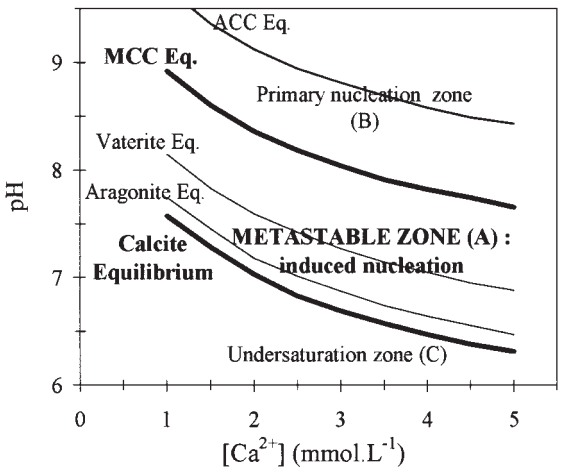


**Figure 12. Demarcation of the metastable zone (A) for the "$CaCO_3$–$CO_2$–$H_2O$" system.**

the solution could be supersaturated with respect to anhydrous forms (vaterite, aragonite, and calcite) without any possibility of spontaneous nucleation. The metastability can be broken by adding $CaCO_3$ seed crystals, and precipitation is induced. In this case, a secondary nucleation supported by the seed crystals takes place.

The predicted model of the metastable zone, in the Ca–carbonic system, is in agreement with experimental results.

## Literature Cited


Bischoff, J. L., J. A. Fitzpatrick, and R. J. Rosenbauer, "The Solubility and Stabilization of Ikaïte ($CaCO_36H_2O$) from 0 to 25°C: Environmental and Paleoclimatic Implications for Thinolite Tufa," *J. Geol.*, **101**, 21 (1993).

Bolze, J., B. Peng, N. Dingenouts, P. Panine, T. Narayanan, and M. Ballauff, "Formation and Growth of Amorphous Colloidal $CaCO_3$ Precursor Particles as Detected by Resolved SAXS," *Langmuir*, **18**, 8364 (2002).

Brecevic, L., and A. E. Nielsen, "Solubility of Calcium Carbonate Hexahydrate," *Acta Chem. Scand.,* **47**, 668 (1993).

Collier, A. P., and M. J. Hounstow, "Growth and Aggregation Rates for Calcite and Calcium Oxalate Monohydrated," *AIChE J.*, **45**, 2298 (1999).

Elfil, H., "Contribution for Study of the South Tunisian Geothermal Waters: Study of Mechanism and Prevention of Scaling Phenomenon," PhD Thesis, INSA Toulouse, France (1999).

Elfil, H., and H. Roques, "Contribution à l'Étude des Phénomènes d'Entartrage. 10ème Partie: Étude de la Signification Physique de la Droite Limite de Précipitation," *Tribune de l'Eau*, **52**, 29 (1999).

Elfil, H., and H. Roques, "Role of Hydrate Phases of Calcium Carbonate on the Scaling Phenomenon," *Desalination*, **137**, 177 (2001a).

Elfil, H. and H. Roques, "Role of Quartz Microbalance in the Study of Calcium Carbonate Germination," *Entropie*, **231**, 28 (2001b).

Gache, N., "Rôles des Formes Hydratées du Carbonate de Calcium dans la Rupture de l'État Métastable des Solutions Sursaturées," PhD Thesis, Université Montpellier II, France (1998).

Gal, J. Y., Y. Fovet, and N. Gache, "Mechanisms of Scale Formation and Carbon Dioxide Partial Pressure Influence. Part I. Elaboration of an Experimental Method and a Scaling Model," *Water Res.*, **36**, 755 (2002).

Gal, J. Y., N. Gache, and Y. Fovet, "Mechanism of Scale Formation and Temperature Influence," *J. Eur. Hydrogeol.*, **31**, 47 (2000).

Greenwald, I., "The Dissociation of Calcium and Magnesium Carbonates and Bicarbonates," *J. Biol. Chem.*, **141**, 789 (1941).

Harmer, W. J., "Theoretical Mean Activity Coefficients of Strong Electrolytes in Aqueous Solutions from 0 to 100°C," *U.S. Natl. Bur. Stand., Ref. Data Ser.*, **24**, 271 (1968).

Johnston, J., H. E. Merwin, and E. D. Williamson, "The Several Forms of Calcium Carbonate," *Am. J. Sci.*, **4**(XLI), 473 (1916).

Koutsoukos, P. G., and C. G. Kontoyannis, "Precipitation of Calcium Carbonate in Aqueous Solutions," *J. Chem. Soc., Faraday Trans.*, **1**(80), 1181 (1984).

Kralj, D., and L. Brecevic, "Dissolution Kinetics and Solubility of Calcium Carbonate Monohydrate," *Colloids Surf. A*, **96**, 287 (1995).

Mersmann, A., *Crystallization Technology Hand Book*, Marcel Dekker, New York (1995).

Mersmann, A., and K. Bartosch, "How to Predict the Metastable Zone Width," *J. Cryst. Growth*, **183**, 240 (1998).

Mulin, J. W., *Crystallization*, Butterworth-Heinemann, London (1993).

Nielsen, A. E., and J. M. Toft, "Electrolyte Crystal Growth Kinetics," *Cryst. Growth*, **67**, 278 (1984).

Ogino, T., T. Suzuki, and K. Sawada, "The Formation and Transformation Mechanism of Calcium Carbonate in Water," *Geochim. Cosmochim. Acta*, **51**, 2757 (1987).

Plummer, L. N., and E. Busenberg, "The Solubilities of Calcite, Aragonite and Vaterite in Solutions between 0 and 90°C, and an Evaluation of the Aqueous Model for the System $CaCO_3$–$CO_2$–$H_2O$," *Geochim. Cosmochim. Acta*, **46**, 1011 (1982).

Reddy, M. M., and G. H. Nancollas, "The Crystallization of Calcium Carbonate. I. Isotopic Exchange and Kinetics," *J. Colloid Interface Sci.*, **36**, 166 (1971).

Reiger, J., J. Thienne, and C. Schmidt, "Study of Precipitation Reactions by X-ray Microscopy: $CaCO_3$ Precipitation and the Effect of Polycarboxylates," *Langmuir*, **16**, 8300 (2000).

Roques, H., *Chemical Water Treatment: Principles and Practice*, VCH, New York (1996).

Roques, H., and A. Girou, "Kinetics of the Formation Conditions of Carbonate Tartars," *Water Res.*, **8**, 907 (1974).

Sheikholeslami, R., "Nucleation and Kinetics of Mixed Salts in Scaling," *AIChE J.*, **49**, 194 (2003).

Tai, C. Y., W. C. Chien, and C. Y. Chen, "Crystal Growth Kinetics of Calcite in a Dense Fluidised–Bed Crystallizer," *AIChE J.*, **45**, 1605 (1999).

Truesdell, A. H., and B. F. Jones, "A Computer Program for Calculating Chemical Equilibria of Natural Waters," *U.S. Geol. Survey J. Res.*, **2**, 233 (1974).

Ulrich, J., and C. Sterge, "Some Aspects of the Importance of the Metastable Zone Width and Nucleation in Industrial Crystallizers," *J. Cryst. Growth*, **237**, 2130 (2002).


*Manuscript received Apr. 8, 2003, and revision received Nov. 17, 2003.*